

Super-X divertors and high power density fusion devices^{a)}

P. M. Valanju,^{1,b)} M. Kotschenreuther,¹ S. M. Mahajan,¹ and J. Canik²

¹*Institute for Fusion Studies, The University of Texas at Austin, Austin, Texas 78712-1060, USA*

²*Oak Ridge National Laboratory, Oak Ridge, Tennessee 37830, USA*

(Received 7 December 2008; accepted 11 March 2009; published online 17 April 2009)

The Super-X Divertor (SXD), a robust axisymmetric redesign of the divertor magnetic geometry that can allow a fivefold increase in the core power density of toroidal fusion devices, is presented. With small changes in poloidal coils and currents for standard divertors, the SXD allows the largest divertor plate radius inside toroidal field coils. This increases the plasma-wetted area by 2–3 times over all flux-expansion-only methods (e.g., plate near main X point, plate tilting, X divertor, and snowflake), decreases parallel heat flux and hence plasma temperature at plate, and increases connection length by 2–5 times. Examples of high-power-density fusion devices enabled by SXD are discussed; the most promising near-term device is a 100 MW modular compact fusion neutron source “battery” small enough to fit inside a conventional fission blanket. © 2009 American Institute of Physics. [DOI: 10.1063/1.3110984]

I. INTRODUCTION

Research in tokamaks has experimentally demonstrated many advances in core confinement physics that can allow core power densities much higher than ITER (International Thermonuclear Experimental Reactor). The main obstacle now in reaching the high power density regime in the next generation long pulse fusion devices is the limited ability of standard divertors (SDs) to simultaneously handle the very high heat and neutron fluxes. The 2007 ITER physics basis¹ clearly states that “fusion gain in steady state maximizes at low density for constant β_N . The limitation on reducing density in next generation tokamaks is set by the impact on the divertor,” and “presently developed advanced scenarios have not yet provided fully integrated scenarios and several issues remain to be solved such as edge compatibility with the divertor.”

We show that one solution to this “divertor bottleneck” problem lies in a redesign of the divertor magnetic geometry. With small changes in poloidal field coil locations and currents for most SD cases, we show how to move the divertor plates to the largest possible radius R_{div} inside toroidal field (TF) coils to create the Super-X Divertor (SXD). We then show how the increase in R_{div} has many positive consequences as follows: (a) it increases the plasma-wetted area by 2–3 times (in proportion to R_{div}) over all flux-expansion-only methods (e.g., plate near main X point, plate tilting, X divertor,² and snowflake³), (b) it increases the magnetic connection length from plasma to divertor plate by 2–5 times, which, through cross-field diffusion can increase the wetted area by a factor of about 1.4, and (c) the magnetic flux tubes broaden at the larger R_{div} , thus decreasing the parallel heat flux and hence the plasma temperature at the divertor plate. The long L and low plasma temperature at the divertor plate allow an increase in radiation near the plate with fewer impurities bleeding back into the main plasma. Together, these

multiplicative improvements can increase the total power that may go into the scrape-off-layer (SOL) by a factor of about 5 while keeping the heat flux on the divertor plate below 10 MW/m². With SXD, the heating power P_h (=auxiliary heating power P_{aux} + 20% of the fusion power P_f) can increase by about five times over the SD. It also allows a decrease in the edge plasma density and the need to radiate—both can lead to better core plasma performance.

We present some examples of SXD equilibria designed using the CORSICA code⁴ and results of two-dimensional (2D) scrape-off layer simulations using the SOLPS code.⁵ Some generic features of SXDs emerge from the following cases: (a) the SXD configuration is relatively easy to design for many plasma aspect ratios, shapes, and core profiles, (b) the necessary coil locations and currents are quite similar to the SD cases, (c) superconducting coils outside the toroidal coils can produce SXDs, (d) the plasma strike point location in SXD is very stable to various plasma perturbations because it depends more on the nearby SXD coils than on the relatively distant plasma current, (e) the plasma temperature at the SXD divertor plates can be dropped below 10 eV at higher power densities, and (f) for double-null cases, the inside divertor plates are not the limiting problem because most of the heat flux goes to the outer plates.

The ability to access the high power density regime opens many possible applications, some of which are discussed here. One possible near-term application is a 100 MW modular compact fusion neutron source (CFNS) “battery” small enough to fit inside a conventional fission blanket. We outline the design parameters, core plasma physics, challenges, and possible payoffs of such a device—for more details we refer the reader in Ref. 6.

II. THE DIVERTOR HEAT FLUX PROBLEM

The *edge* geometry of the magnetic bottle can have a major impact on *core* plasma. Divertors increase the isolation of the core plasma from material regions of maximum heat flux, which improves core confinement. The *H*-mode first

^{a)}Paper T12 2, Bull. Am. Phys. Soc. 53, 240 (2008).

^{b)}Invited speaker. Electronic mail: pvalanju@mail.utexas.edu.

appeared in tokamaks with divertors. However, because transport along magnetic surfaces is much faster than across them, the heat flux necessarily concentrates strongly on divertor plates. Material and engineering constraints limit the maximum heat flux that a divertor plate can handle to about 10 MW/m^2 . For a given divertor geometry, this limits the maximum heat flux that can be put into the SOL, which, in turn, limits the maximum power density in the core. This did not become a limiting problem until the plasma core confinement and methods to inject power were improved to the levels now attained in existing devices.⁷ Some current devices can now reach (and exceed for short times) the 10 MW/m^2 limit. ITER divertor is near this limit and the next generation of devices will be operated at higher power densities. The estimate P_h/R (R =plasma major radius) is often used as a measure of the severity of the heat flux problem.⁸ Table I of Ref. 2 showed that the P_h/R will be about 5–6 times ITER for steady-state fusion reactors^{9–12} and 2–4 times ITER for most next generation experiments.^{13–15} The increases in P_h are large in going from the two largest current tokamaks [JET in European Union (EU) with major radius $R=3 \text{ m}$ and JT-60 in Japan with $R=3.4 \text{ m}$, each with $P_h \sim 20 \text{ MW} > P_f$] to ITER ($R=6.2 \text{ m}$, designed for $P_h = 120 \text{ MW} < P_f \sim 400\text{--}500 \text{ MW}$), and again in going from ITER to even a moderate power fusion reactor ($P_h \sim 400\text{--}720 \text{ MW}$, $P_f \sim 2000\text{--}3600 \text{ MW}$).

A detailed analysis² showed that any attempt to save the SD by injecting impurities to radiate power would lead to too many impurities in the core and thus destroy good core confinement at high β —an unacceptable outcome. A basic redesign of the divertor magnetic geometry to (a) spread the heat flux over a larger plate area and (b) to increase the magnetic distance to the divertor plates to increase divertor-plasma isolation and decrease plasma temperature at the plates, thus possibly allowing more radiation in the divertor, is therefore indicated.

III. THE SUPER-X DIVERTOR

Neglecting cross-field diffusion, the plasma-wetted area A_w at radius R_{div} on the divertor plates is approximately given by (using $\nabla \cdot \mathbf{B} = 0$)

$$A_w = \frac{B_{p,\text{SOL}}}{B_{\text{div}}} \frac{A_{\text{SOL}}}{\sin(\theta)} \approx \left[\frac{B_p}{B_t} \right]_{\text{SOL}} \frac{R_{\text{div}}}{R_{\text{SOL}}} \frac{A_{\text{SOL}}}{\sin(\theta)}, \quad (1)$$

where $B_{p,\text{SOL}}$, R_{SOL} , and A_{SOL} are the poloidal field, radius, and heat flux area of the SOL at the midplane and $\theta = \tan^{-1}(B_{\perp}/B_t)$ is the angle between the divertor plate and the total magnetic field B_{div} at the plate ($B_{\perp} = \mathbf{B}_p \cdot \hat{\mathbf{n}}$ is the field normal to the plate). The subscripts $p(t)$ denote the poloidal (toroidal) directions.

The simplest way to increase the plasma-wetted area A_w is to tilt the plate so as to decrease B_{\perp} and hence θ . Another way is to expand the flux at the plates by decreasing the poloidal field B_p at the plate. Both decrease B_{\perp} . Flux expansion can be done by moving the plates near the main plasma X points, by using pairs of poloidal coils to locally decrease the poloidal field (the X divertor²), or by increasing the order of the main X point (the snowflake divertor³). However, all

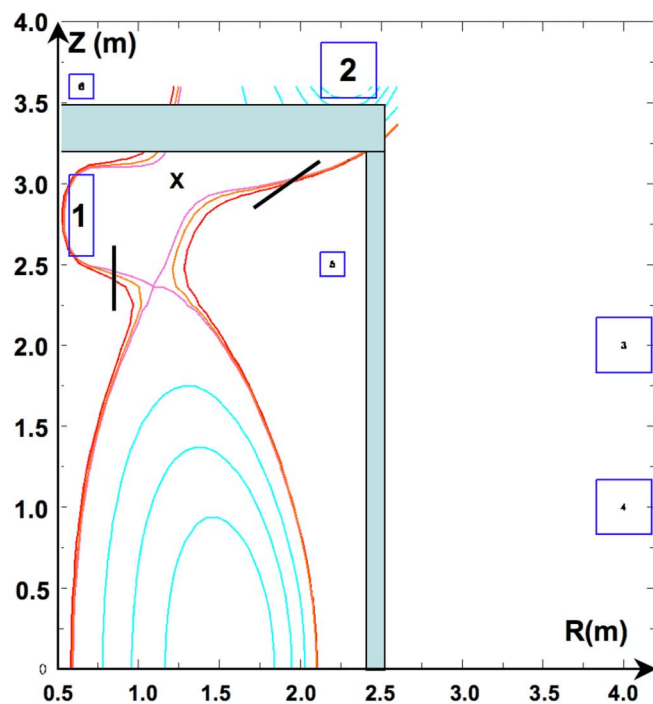
these methods are limited because θ cannot be arbitrarily small. The generally accepted minimum is 1° (Ref. 16) (ITER θ is 2.3°) because even small divertor plate irregularities become problematic at lower θ . Under this $\theta > 1$ restriction, the heat capacities of all the above methods remain far below the demands of the next generation high power density devices.

Thus, for a given W_{SOL} and B_p/B_t at the midplane SOL (set by the core plasma), the only way to increase A_w is by moving the divertor plate to a larger major radius R_{div} . The basic idea of the SXD is to maximize R_{div} by using only axisymmetric poloidal field coils. In addition, the magnetic line length L from the SOL midplane to the divertor plate can also be increased by decreasing the poloidal field in the long divertor leg at large R . Large R_{div} also reduces the parallel heat flux q_{\parallel} on the plates because the area of each flux tube increases as the total B decreases. Large R_{div} , long L , and low q_{\parallel} at the plates are generically obtained in SXDs with extra X points—a method similar to the X divertor;² hence the name SXD.

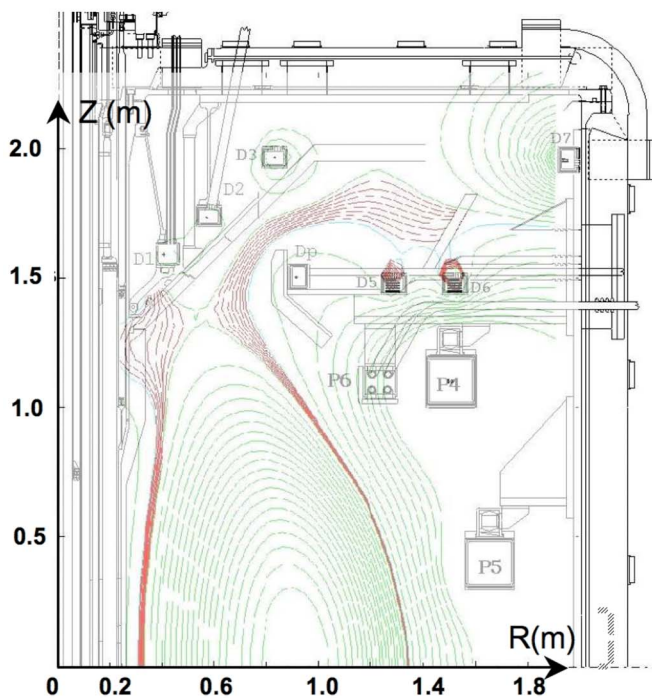
We use the CORSICA magnetic equilibrium code⁴ to design the SXD equilibria. Two examples are shown in Fig. 1. SXDs can be generated from SD equilibria by the following generic method. Noting that each main X point in a SD case is made essentially with a main divertor coil to cancel the poloidal field of the plasma current, a SXD can be made by splitting the main divertor coil into two (with nearly the same total current) and moving one of them to larger major radius. In general an extra X point appears between the two [see “x” in Fig. 1(a)] and magnetic surfaces just outside the separatrix now wind around the two coils. This pulls the SOL out to larger major radii, thus generating the SXD. This generic method qualitatively explains why the total SXD coil currents are about the same as for the SD in all the cases we have studied and why SXDs can be made for plasma shapes and profiles. The SXD configuration can then be optimized by further splitting the SXD coils, as shown in Fig. 1(b); flux can be expanded (by decreasing the poloidal field) all along the long SXD legs, leading to longer connection lengths. The SXD design space is found to be smooth, versatile, and quite robust (to small plasma and coil changes).

Using CORSICA, we have found SXD equilibria for many devices where SXD could be crucial including (a) tokamaks with copper coils: aspect ratios $A=1.4$ for a component test facility (CTF),¹³ $A=1.4$ for the Mega Amp Spherical Tokamak (MAST),¹⁷ $A=1.8$ for the National Spherical Tokamak Experiment (NSTX),¹⁸ the National High-Power Tokamak Experiment (NHTX),¹⁴ one variant of $A=2.0$ CFNS,⁶ the $A=3.5$ Fusion Development Facility (FDF) (Ref. 15) and (b) tokamaks with superconducting coils all outside the TF coils: $A=2.6$ for the SLIMCS reactor¹¹ and $A=4$ for ARIES-AT.¹⁰ Various gains due to SXD are summarized in Table I and two examples are shown in Fig. 1 (most SXD equilibria look similar to these two).

In general, SXDs are found to be easy to obtain for all plasma shapes and parameters examined. In existing devices, SXD gains are limited by existing constraints such as pumping ducts, supports, vacuum vessel shapes, etc. For each device, the basic SXD design procedure is refined by further



(a)



(b)

FIG. 1. (Color online) Two examples of SXD CORSICA equilibria for (a) a high power density CFNS and (b) MAST upgrade.

splitting the two coils and fine tuning their locations and currents to produce sequences of configurations (e.g., CTF1, CTF2 or FDF1, FDF2, FDF3, etc.) that fit various constraints specific to each case. For all cases, in going from standard to superdivertor, the total ampere meters in the SXD poloidal field coils change by less than $\pm 5\%$ while the core plasmas remain essentially unaffected.

One generic but nonobvious advantage of SXD is that the strike point location is *less* sensitive to plasma fluctuations for SXD than for SDs. The strike point geometry depends more on nearby SXD coils than on faraway plasma current. For example, for the NHTX case, changing the plasma current by $\pm 3\%$ moves the outer strike point only by ± 0.5 cm, a small fraction of the width of the plasma-wetted area (11 cm), and much less than the movement of the main X point (± 2.8 cm).

In most SXD cases (from the low aspect ratio NHTX and CTF to high aspect ratio FDF, as well as superconducting reactors SLIM-CS and ARIES-AT) we have found a natural “fit” for the long SXD legs in corners of the TF coils—these corners are typically not used. If the SXD is deemed essential to make a high power density device work at all, one would have to make room for it inside the TF coils. Given the significant advantages of SXD, the extra cost of TF “real estate” seems reasonable. Details of such tradeoffs will, of course, be system design issues.

IV. SXD GAINS

In addition to increasing the plasma-wetted area A_w in proportion to R_{div} , the SXD method of using an extra X point allows a significant increase in the connection length (along B) from the plasma to the divertor plate. Since the SOL widths are about 1 cm in many devices, we measure the connection length L along a line that starts at 1/2 cm outside the separatrix in the midplane. Table I shows the range of improvements in L and A_w for some of the SXD configurations we have designed. The SXD line lengths are ~ 2 – 5 times greater than the line lengths L_x to the main X point. As shown by the CTF1-2 and the FDF1-2-3 series in Table I, L can be further increased by refining the SXD coil(s), e.g., by splitting the SXD coil into two or four coils, such that the total current is the same.

Increasing L further increases A_w through cross-field diffusion. Standard models of SOL diffusive processes [see Ref. 19, p. 269, Eq. (5.79)] indicate the SOL width scales with the connection length as $L^{2/9}$, leading to an increase in A_w by about 1.4. Although details of the divertor region turbulence and flux variation along the line may make this factor higher or lower, this rough estimate is useful during SXD design explorations.

Radiation can further decrease the power incident on the divertor plate but only if the plasma does not “burn through,” i.e., the temperature at the divertor plates stays low. If a fraction f_{rad} of the power can be radiated away from the divertor plates, these three effects together can give an estimated gain in the maximum power allowed into the SOL of $P_{\text{gain}} = (R_{\text{div}}/R_x)(L/L_x)^{2/9}/(1-f_{\text{rad}})$, where R_x is the radius of the main X point and L_x is the line length up to a point at the same z as the main X point. Since the location of the SD is generally near the main X point (with some variability from device to device), we use the main X point to define a uniform measure P_{gain} . Although it slightly overestimates the SXD gain over SDs, it is useful as a rough estimate before detailed simulations and in SXD design optimization loops.

TABLE I. SXD geometrical gains for some of the cases. The devices are listed in the text. The last row shows the approximate expected SXD gain P_{gain} in power handling. With SXD, the plasma temperature at the plate is low enough that about 50% power can be radiated away from the divertor plate ($f_{\text{rad}}=0.5$) as verified by SOLPS.

	NHTX	CFNS	SLIMCS	ARIES	CTF1	CTF2	DFD1	DFD2	DFD3
R_{div}/R_x	2.9	1.9	1.6	1.7	2.7	2.8	1.9	1.9	1.9
$L[m]$	38	53	78	66	27	37	62	67	74
L/L_x	3.4	3.0	2.7	1.9	2.1	2.7	4.0	4.2	4.7
$A_w[m^2]$	5.3	7.9	7.0	8.2	10.4	9.8	5.6	5.7	5.6
P_{gain}	7.6	4.8	4.0	4.0	6.4	7.1	5.1	5.2	5.2

For example, for the NHTX case in Fig. 2 and column 1 of Table I, P_{gain} estimate is 7.6 while SOLPS gives 7.2.

To estimate whether a divertor (standard or SXD) will be in the sheath limited regime, i.e., whether the plasma will burn through to the divertor plate so that the plasma temperature at the plate will be over 100 eV or so, we use the sheath parameter²¹ $S = Q_{\parallel u}(B_{\text{div}}/B_u)/n^{1.75}L^{0.75}/3 \times 10^{-27}$, which we have successfully benchmarked against 2D SOLPS code results. The plasma burns through if $S > 1$. Here the upstream (u) parallel heat flux $q_{\parallel u} = P_{\text{SOL}}/4\pi R_u \lambda_q (B_p/B)_u$, where λ_q is the SOL power width. We find that the sheath parameter S is above 1 for most of the high power density SDs but below 1 with SXD.

We use the SOLPS code to calculate the peak heat flux on the divertor plate and plasma temperature T_{plt} at the location of the peak heat flux. The total power into the SOL and the edge density are inputs to the code. In general,²⁰ we find that SXD is able to keep the heat flux on the divertor below 10 MW/m² and the temperature at the plate low (near 10 eV). The plasma temperature T_{plt} at the location of the peak heat flux on the plate determines whether radiation will be effective. SOLPS also confirms that adding impurities gives very little radiation if T_{plt} is high (well above 100 eV), as is found for most SD cases at high P_h/R . In contrast, as in Fig. 2, 50% of the power can be radiated with SXD only because T_{plt} is low enough for impurities to radiate. Note that the radiation mostly occurs close to the divertor plate where the plasma temperature is low, so about half of it still falls on the divertor plate, so maximum f_{rad} is about 1/2. Low T_{plt} also reduces adverse plate-plasma interactions like sputtering, plate damage, etc.

The canonical problem with augmenting the heat handling capacity of divertors with impurity radiation is that impurities injected in the divertor also contaminate the core plasma. The extreme isolation of the SXD from the plasma can minimize this problem, thus enhancing the maximum divertor radiation fraction.

Figure 2 shows the SOLPS calculations for NHTX.¹⁴ From column 1 of Table I and the discussion above, one expects a decrease in peak heat flux by a factor of about $2.89 \times 3.4^{2/9} \times 2 = 7.6$ (from increases in R_{div} and L and 50% carbon radiation), which agrees well with the SOLPS result (7.2) in Fig. 2(a).

In general, SOLPS runs confirm that the SD is rather inadequate for any high power density machine. The peak heat flux stays well above 10 MW/m² and T_{plt} stays at around 150 eV so that almost no impurity radiation is possible. Ba-

sically, the parallel heat flux q_{\parallel} into the divertor is so large that the plasma just burns through a SD (Ref. 21)—SDs are always deep in the sheath limited regimes for high power density devices. As far as we know, only the SXD can cure this problem.

V. FURTHER SXD ISSUES

A new idea like SXD is naturally expected to raise many new issues. An oft raised issue with SXD is the inner divertor. Almost all of high power density devices in the future plan to use a double-null configuration because of the high divertor heat load and perhaps because the experimental ability for plasma control has significantly improved. In such double-null cases, the inner divertor is not a major concern because the typical ratio of heat flux to outer and inner divertors is over 5 to 1 (usually closer to 10 to 1).²² This split is also seen in our SOLPS simulations. Also, the SXD does not increase the heat flux on the inner divertor plate while decreasing it on the outer divertor plate. Thus, unless SXD is needed to raise the power density by over five times, the outer divertor still is the limit.

Another set of questions is about the relative importance of parallel versus cross-field transport in the long SXD legs. In general, an increase in cross-field transport (by whatever mechanism) will be good—it will increase the wetted area and thus reduce the peak heat flux. We also generally make sure that the long SXD leg does not pass too near the extra X point so that ergodic layers creating hot spots on the target are not expected to be a problem, although this needs to be confirmed with three-dimensional calculations in the future.

The SXD suggests many further speculations to explore and test by simulations and/or experiments. (1) The long L and nonmonotonic poloidal field along the SXD may allow stable detached operation. (2) One may be able to enhance the turbulence in the long SXD leg without it bleeding back to the main plasma. (3) Because of the longer SXD connection length, transient heat flux pulses such as edge localized modes (ELMs) from the plasma may have less impact on the SXD. The increased wetted area of the SXD will spread ELM pulses over a larger area and the longer line length will spread it over time, both of which can greatly reduce the damage, but this needs confirmation. (4) The ability of SXD to handle more heat flux allows lower density at the edge, cleaner plasma, and higher power flow through any edge barriers, as verified by SOLPS results. This may enable dependable access to the high β regime. Operating at rather

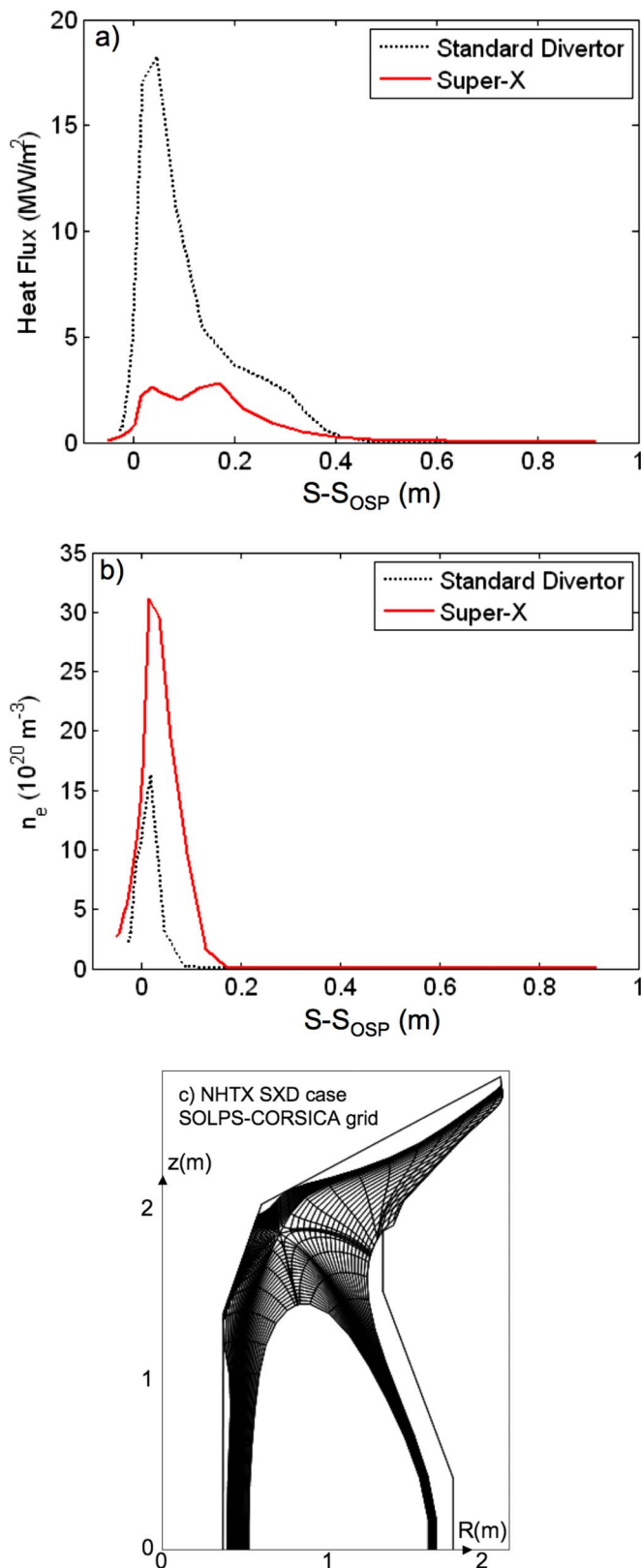


FIG. 2. (Color online) SOLPS results for NHTX SD (black, dotted) and SXD (red, solid) equilibria showing (a) over fivefold decrease (by about 7.2 in this case) in total peak divertor heat flux (includes radiation falling back on divertor plate) and (b) a twofold increase in the density at the divertor plate. The SOLPS grid (based on NHTX CORSICA equilibrium for SXD) used in these calculations is shown in (c). Simulation parameters are input power = 50 MW, density at the core boundary = $1.5 \times 10^{20} \text{ m}^{-3}$, carbon impurity, same tilt angle θ (1°) for both SD and SXD cases.

low edge densities enhances the core density gradients that result in much higher bootstrap current, possibly allowing much higher β for the same β_n [set by magnetohydrodynamic (MHD) stability]. In addition to increasing bootstrap current,²¹ lower density also increases the current drive efficiency.¹ One could also operate with a very high pedestal temperature only because the SXD can handle the enhanced heat load. At this point, all these are plausible speculations that need to be tested using coupled core-edge simulations. (5) Helium exhaust drops precipitously with neutral pressure. The high temperature at the divertor plate in non-SXD geometries often leads to low recycling and hence low neutral pressures. This makes He pumping difficult. Also, the resulting long mean path would imply very low transconductance through any reasonable pumping duct. Further, in SXD the distances from pumps at larger major radii can be shorter and the pumping area at larger R_{div} can be higher. Whether these translate into He pumping advantages needs to be checked. Some of these issues will be checked on experiments like MAST, NSTX, and DIII-D which plan to test SXD.

VI. NEUTRON FLUX CALCULATIONS FOR SXD

Another critical problem that only SXD can probably solve is simultaneous heat and neutron damage to the divertor plate. The long legs of the SXD also allow significant shielding of the SXD plates from neutrons. Such shielding does not appear feasible for the SDs or any of the flux-expanded divertors. The divertor plate has to use materials that have high thermal conductivity as substrates to be able to withstand and extract the enormous heat, for example, tungsten armor on a high conductivity copper substrate or copper and carbon composites. Such materials severely deteriorate after only a few displacements per atom (dpa) due to neutron bombardment. For copper alloys, the temperature window between brittleness and creep strength is too narrow; carbon-based materials swell and degrade in thermal conductivity. Only hypothetical materials might be able to withstand the 50–100 dpa as well as high heat that a SD will have to face to last long enough to be credible. Therefore, it is critical to shield the divertor from neutrons. We have performed calculations using the Monte Carlo MCNPX (Ref. 23) code (widely used to design fission reactors) to show that for a typical SXD configuration, the neutron flux on the plate can be reduced by a factor of 10 or more. Only with such shielding could much of the divertor technology already developed for ITER be transferable to high duty cycle deuterium-tritium operation in component test facilities or CFNS for fusion-fission hybrid applications.

VII. COMPACT FUSION NEUTRON SOURCE

Two possible mission directions are suggested for SXD-enabled, small high power density tokamaks. (1) One could design a CTF to fulfill a short-term, useful, and necessary fusion development task. Because of SXD, this could be done parallel to ITER using only conservative physics and technology. As a by-product, one will develop a CFNS that also has many advantages as the neutron driver in a fusion-fission hybrid, as discussed in Ref. 6. (2) Alternatively, one

can develop or modify existing devices to test advanced physics operating modes for a pure fusion reactor in an integrated fusion environment with high heat fluxes.

As an example of the first type, we now consider a compact high power density device using SXD. The goal is to reach high power densities but stay conservatively well within known physics and technology limits so that a test device could, in principle, be built in near term. To keep the size, coil mass, and cost small ($R \sim 1.35$ m), and for ease of maintenance, we choose low aspect ratio ($A \sim 1.8$, which is near cost minimum in studies) spherical tokamak (ST) reactor designs with copper coils and enough room (about 0.1 m) to shield the inboard toroidal coil. The field at the toroidal coil is kept below 7 T. The B field on plasma axis will be 2.5 T. For high performance, we will try to get to high elongation up to $\kappa \sim 3$. The machine is to produce about 100 MW of fusion power and a CTF-class neutron wall load of about 0.93 MW/m².

The two key dimensionless parameters are normalized beta $\beta_N = (\langle p \rangle / B^2) / (I / aB)$ and H factor [confinement improvement over the ITER98H(y,2)] scaling law. The no-wall stability limit is $\beta_N \sim 3$ and getting H much above 1.2 is hard at present. Hence we will stay below these limits. The current drive power for 100 MW of fusion power at a given β_N can be estimated from the current drive efficiency formula $I_n R / P_h \sim 0.3 \times 10^{20} (\langle T_e \rangle / 10 \text{ keV}) \text{ A/W m}^2$, which is very close to what is found in reactor studies and ITER analysis. We use equilibria with fixed temperature and density profiles (characteristic of H -modes) to get β_N , bootstrap current, and fusion power.

We find that for all relevant SOL densities, the sheath parameter S for CFNS remains well above 1 for all but the SXD cases.²¹ Thus, only SXD allows such a device to operate without destroying the divertor. Further, SXD also allows operation at edge densities well below (1/3) the Greenwald limit, thus reducing chances of disruptions. The current drive power is also lowered to about 50 MW at lower densities and the H -factor can be higher (up to about 1.2). Thus SXD enables the necessary plasma operation to produce 100 MW of fusion power in such a small device. The elongation of CFNS is consistent with the present experimental results and is similar to that in other possible future devices, i.e., NHTX, ARIES, and FDF.

MCNPX calculations for this device show that the neutron damage to the center post (with 10 cm steel cladding) and divertor plate can both be kept well below 1 and 2 dpa per full-power year, so that one could operate the device for about 1–2 full power year before serious repairs. During this time, the device can produce about 0.93 MW/m² neutron wall load that can be used for fusion-fission hybrid as well as component testing applications.

VIII. CONCLUSION AND FUTURE DIRECTIONS

In summary, the SXD improves divertor performance in many ways. While obeying the $\theta = 1^\circ$ plate-tilt limit, it increases the plasma-wetted area by about 1.5–3. The poloidal B field in the long divertor leg can be decreased to increase the line length L by about two to five times and increase SOL

width via diffusion by about a factor of 1.4. The flux tubes broaden at larger R_{div} , lowering the q_{\parallel} at the plates, which lowers plasma temperature at the plate to below 10 eV and increases the maximum divertor radiation fraction up to 50% as verified by SOLPS. All these enhancements are multiplicative, so the maximum P_{SOL} that can be put into the SXD could go up by a factor of 5 or so as compared to any other purely flux-expanding configuration. This is verified by SOLPS simulations. Such enhancements are important for next generation high power density devices.

By maximizing the isolation (both physical and magnetic) between the core plasma and the divertor SOL, the SXD allows both to be better optimized. It increases plasma-wetted area and line length to simultaneously solve the divertor heat flux problem, shield the divertor from neutron damage, and enable reactor-relevant core beta values with acceptable heat exhaust—all with axisymmetric poloidal field coils that are not very different from those for SDs. No other divertor configuration that we know simultaneously does all these.

ACKNOWLEDGMENTS

We thank R. H. Bulmer, L. D. Pearlstein, R. Maingi, M. Istenic, and R. Buttery. Support from U.S. DOE (Grant Nos. DE-FG02-04ER54742 and DE-FG02-04ER54754) is acknowledged.

- ¹“Progress in the ITER Physics Basis,” Special Issue, Nucl. Fusion **47**, 6 (2007).
- ²M. Kotschenreuther, P. Valanju, and S. Mahajan, Phys. Plasmas **14**, 072502 (2007).
- ³D. Ryutov, Phys. Plasmas **14**, 06452 (2007).
- ⁴J. A. Crotinger, L. L. LoDestro, L. D. Pearlstein, A. Tarditi, T. A. Casper, and E. B. Hooper, LLNL Report No. UCRL-ID-126284, 1997.
- ⁵R. Schneider, X. Bonnin, K. Borrass, D. P. Coster, H. Kastelewicz, D. Reiter, V. A. Rozhansky, and B. J. Braams, Contrib. Plasma Phys. **46**, 3 (2006).
- ⁶M. Kotschenreuther, P. Valanju, S. Mahajan, and E. Schneider, Fusion Eng. Des. **84**, 83 (2009).
- ⁷J. Wesson, Tokamaks, 3rd ed. (Oxford University Press, Inc., New York, 2004), pp. 561–704.
- ⁸K. Lackner, Comments Plasma Phys. Controlled Fusion **15**, 359 (1994); P. J. Catto, D. A. Knoll, and S. I. Krasheninnikov, Phys. Plasmas **3**, 191 (1996).
- ⁹I. Cook, N. Taylor, and D. Ward, 20th IEEE/NPSS Symposium on Fusion Engineering (SOFE), San Diego, 14–17 October 2003.
- ¹⁰“ARIES reactor studies,” Special Issue, Fusion Sci. Technol. **54**, 3 (2008).
- ¹¹M. Sato, S. Sakurai, S. Nishio, K. Tobita, T. Inoue, Y. Nakamura, K. Shinya, and H. Fujieda, Fusion Eng. Des. **81**, 1277 (2006).
- ¹²K. Okano, Y. Asaoka, T. Yoshida, M. Furuya, K. Tomabechi, Y. Ogawa, N. Sekimura, R. Hiwatari, T. Yamamoto, T. Ishikawa, Y. Fukai, A. Hatayama, N. Inoue, A. Kohyama, K. Shinya, Y. Murakami, I. Senda, S. Yamazaki, S. Mori, J. Adachi, and M. Takemoto, Nucl. Fusion **40**, 635 (2000).
- ¹³Y.-K. M. Peng, P. J. Fogarty, T. W. Burgess, D. J. Strickler, B. E. Nelson, J. Tsai, C. A. Neumeyer, R. Bell, C. Kessel, J. Menard, D. Gates, B. LeBlanc, D. Mikkelsen, E. Fredrickson, L. Grisham, J. Schmidt, P. Rutherford, S. Sabbagh, A. Field, A. Sykes, I. Cook, O. Mitarai, and Y. Takase, Plasma Phys. Controlled Fusion **47**, B263 (2005); Y. K. M. Peng, T. W. Burgess, A. J. Carroll, C. L. Neumeyer, J. M. Canik, M. J. Cole, W. D. Dorland, P. J. Fogarty, L. Grisham, D. L. Hillis, Y. Katoh, K. Korsah, M. Kotschenreuther, R. LaHaye, S. Mahajan, R. Majeski, B. E. Nelson, B. D. Patton, D. A. Rasmussen, S. A. Sabbagh, A. C. Sontag, R. E. Stoller, C.-C. Tsai, P. Valanju, J. C. Wagner, and G. L. Yoder, “Extensive remote handling and conservative plasma conditions to enable fusion nuclear science R and D using a component testing facility,” Nucl. Fusion (to be published).

- ¹⁴R. Goldston, J. E. Menard, J. P. Allain, J. N. Brooks, J. M. Canik, R. Doerner, G.-Y. Fu, D. A. Gates, C. A. Gentile, J. H. Harris, A. Hassanein, N. N. Gorelenkov, R. Kaita, S. M. Kaye, M. Kotschenreuther, G. J. Kramer, H. W. Kugel, R. Maingi, S. M. Mahajan, R. Majeski, C. L. Neumeyer, R. E. Nygren, M. Ono, L. W. Owen, S. Ramakrishnan, T. D. Rognlien, D. N. Ruzic, D. D. Ryutov, S. A. Sabbagh, C. H. Skinner, V. A. Soukhanovskii, T. N. Stevenson, M. A. Ulrickson, P. M. Valanju, and R. D. Woolley, "An experiment to tame the plasma material interface," *Nucl. Fusion* (to be published).
- ¹⁵R. D. Stambaugh, V. S. Chan, and C. P. C. Wong, *Bull. Am. Phys. Soc.* **52**, NP8.00123 (2007).
- ¹⁶A. Herrmann, *Plasma Phys. Controlled Fusion* **44**, 897 (2002).
- ¹⁷G. F. Counsell, R. J. Akers, L. C. Appel, D. Applegate, K. B. Axon, Y. Baranov, C. Brickley, C. Bunting, R. J. Buttery, P. G. Carolan, C. Challis, D. Ciric, N. J. Conway, M. Cox, G. Cunningham, A. Darke, A. Dnestrovskij, J. Dowling, B. Dudson, M. R. Dunstan, E. Delchambre, A. R. Field, A. Foster, S. Gee, M. P. Gryaznevich, P. Helander, T. C. Hender, M. Hole, D. H. Howell, N. Joiner, D. Keeling, A. Kirk, I. P. Lehane, S. Lisgo, B. Lloyd, F. Lott, G. P. Maddison, S. J. Manhood, R. Martin, G. J. McArdle, K. G. McClements, H. Meyer, A. W. Morris, M. Nelson, M. R. O'Brien, A. Patel, T. Pinfold, J. Preinhaelter, M. N. Price, C. M. Roach, V. Rozhansky, S. Saarelma, A. Saveliev, R. Scannell, S. Sharapov, V. Shevchenko, S. Shibaev, K. Stammers, J. Storrs, A. Sykes, A. Tabasso, S. Tallents, D. Taylor, M. R. Tourmianski, A. Turner, G. Turri, M. Valovic, F. Volpe, G. Voss, M. J. Walsh, J. R. Watkins, H. R. Wilson, M. Wisse, and MAST, NBI, ECRH Teams, *Nucl. Fusion* **45**, S157 (2005).
- ¹⁸M. Ono, S. M. Kaye, Y.-K. M. Peng, G. Barnes, W. Blanchard, M. D. Carter, J. Chrzanowski, L. Dudek, R. Ewig, D. Gates, R. E. Hatcher, T. Jarboe, S. C. Jardin, D. Johnson, R. Kaita, M. Kalish, C. E. Kessel, H. W. Kugel, R. Maingi, R. Majeski, J. Manickam, B. McCormack, J. Menard, D. Mueller, B. A. Nelson, B. E. Nelson, C. Neumeyer, G. Oliaro, F. Paoletti, R. Parsells, E. Perry, N. Pomphrey, S. Ramakrishnan, R. Raman, G. Rewoldt, J. Robinson, A. L. Roquemore, P. Ryan, S. Sabbagh, D. Swain, E. J. Synakowski, M. Viola, M. Williams, J. R. Wilson, and NSTX Team, *Nucl. Fusion* **40**, 557 (2000).
- ¹⁹P. C. Stangeby, *The Plasma Boundary of Magnetic Fusion Devices* (Taylor & Francis, London, 2000).
- ²⁰J. M. Canik, R. Maingi, L. Owen, J. Menard, R. Goldston, M. Kotschenreuther, S. Mahajan, and P. Valanju, PSI Conference, 2008.
- ²¹M. Kotschenreuther, P. Valanju, S. Mahajan, L. J. Zheng, L. D. Pearlstein, R. H. Bulmer, J. Canik, and R. Maingi, "The Super X Divertor (SXD) and High Power Density Experiment (HPDX)," *Nucl. Fusion* (to be published).
- ²²A. W. Leonard, *Fusion Sci. Technol.* **48**, 1083 (2005).
- ²³J. S. Hendricks, G. W. McKinney, J. W. Durkee, J. P. Finch, M. L. Fensin, M. R. James, R. C. Johns, D. B. Pelowitz, L. S. Waters, and F. X. Gallmeier, Los Alamos National Laboratory Report No. LA-UR-06-7991, 2006.